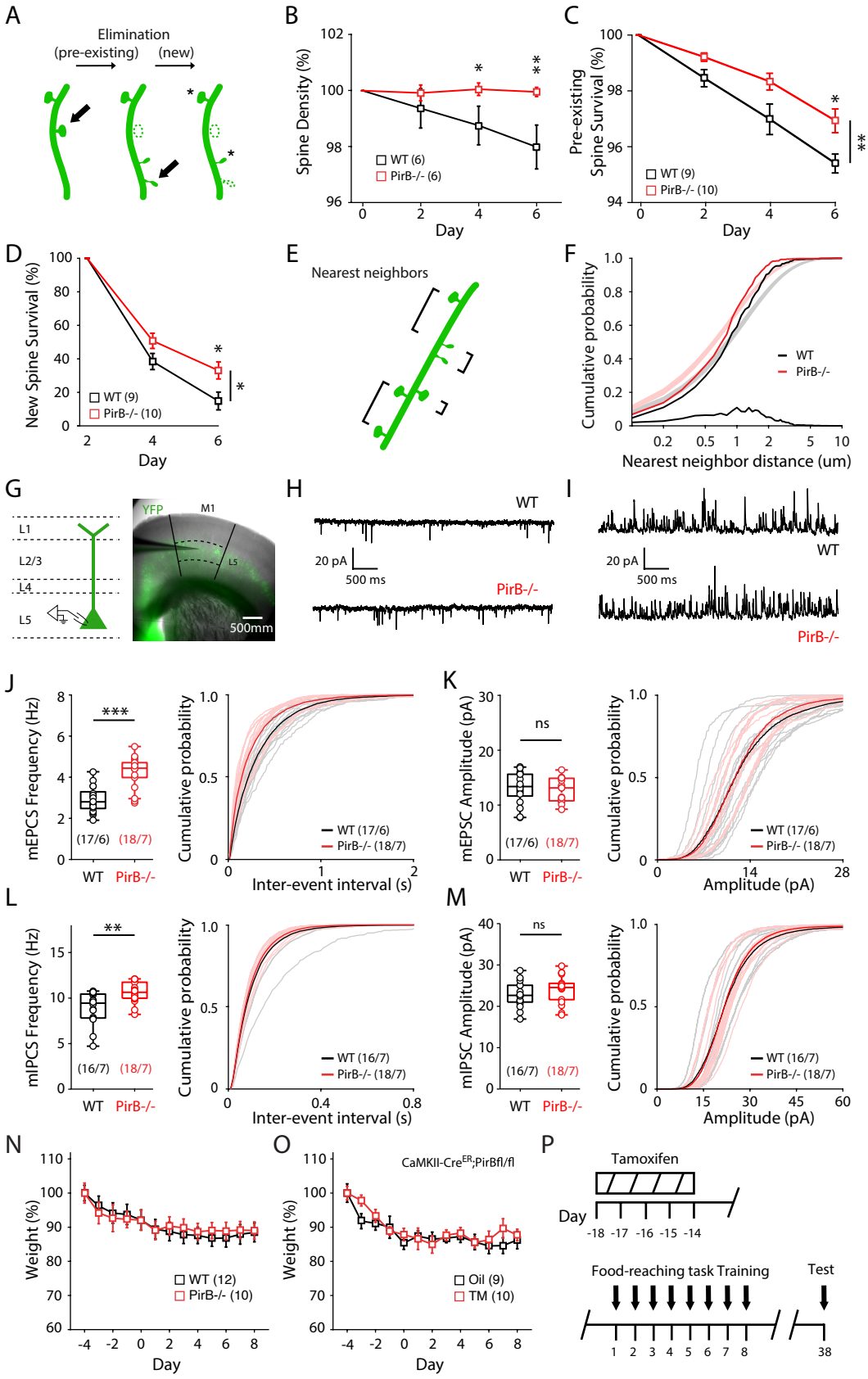

Albarran et al.,- Figure S1

Figure S1 (related to Figure 1). Spine dynamics, basal synaptic transmission, and animal body weights of WT and PirB-/- mice

(A) Depiction of spine elimination involving pre-existing spines (those existing upon the first imaging session) vs. new spines (those formed any day starting the second imaging session).

(B) Spine density (normalized to the first imaging session) declines significantly less over days in PirB-/- mice (WT: n = 6; PirB-/-: n = 6; day 2, WT: 99.37 ± 0.29%, PirB-/-: 99.92 ± 0.12%, p = 0.8182; day 4, WT: 98.75 ± 0.29%, PirB-/-: 100.05 ± 0.09%, p = 0.0455; day 6, WT: 97.98 ± 0.32%, PirB-/-: 99.96 ± 0.07%, p = 0.0043, Mann-Whitney).

(C) Pre-existing spine survival, quantified as the % of spines identified on the first imaging session that were present in subsequent imaging sessions. Greater survival of pre-existing spines in PirB-/- mice compared to WT (WT: n = 9; PirB-/-: n = 10; p = 0.0093, 2-way repeated measures ANOVA). Individual day statistics (day 2, WT: 98.47 ± 0.31%, PirB-/-: 99.22 ± 0.15%, p = 0.0653; day 4, WT: 97.01 ± 0.54%, PirB-/-: 98.35 ± 0.30%, p = 0.0789; day 6, WT: 95.43 ± 0.34%, PirB-/-: 96.95 ± 0.42%, p = 0.022, Mann-Whitney).

(D) New spine survival, quantified as the % of spines identified on the second imaging session that were later present in subsequent imaging sessions. Greater survival of new spines in PirB-/- mice compared to WT (WT: n = 9; PirB-/-: n = 10; p = 0.031, 2-way repeated measures ANOVA). Individual day statistics (day 4, WT: 38.42 ± 4.82%, PirB-/-: 50.76 ± 4.54%, p = 0.1273; day 6, WT: 14.86 ± 5.31%, PirB-/-: 33.10 ± 5.09%, p = 0.0499, Mann-Whitney).

(E) For each spine, the distance to its nearest neighbor (NN) was identified in order to quantify spine clustering along dendrites.

(F) Cumulative distributions were generated for NNs across all spines of both genotypes (solid lines). NNs drawn from shuffled data were used to generate expected random distributions (shaded regions). Both WT and PirB-/- mice spines had significantly more clustering than expected, with more spines represented in the 1-3μm range (WT: n = 3158 spines / 7 mice; p = 9.3e-19; PirB-/-: n = 3986 spines / 8 mice; p = 2.1e-26, 2-sample Kolmogorov-Smirnov). Furthermore, spine NNs in PirB-/- were significantly smaller than those of WT (p = 1.0e-18, 2-sample Kolmogorov-Smirnov), with a greater frequency of spines with 0.2-2.0μm separation (bottom black line).

(G) Acute coronal slices prepared from 2-month old WT or PirB-/- mice crossed to the Thy1-YFP-H+ line. YFP expression allowed for targeting of layer 5 pyramidal neurons for whole-cell patch clamp recordings.

(H) Representative recordings of mEPSCs from M1 layer 5 pyramidal neurons WT and PirB-/- mice. Tetrodotoxin (1μM) and picrotoxin (100μM) were included in the ACSF.

(I) Representative recordings of mIPSCs from M1 layer 5 pyramidal neurons WT and PirB-/- mice. Tetrodotoxin (1μM), NBQX (10μM), and R-CPP (10μM) were included in the ACSF.

(J) The frequency of mEPSCs was significantly increased (decreased inter-event interval) in PirB-/- mice, compared to WT littermates (WT: 3.151 ± 0.148; n = 17 cells / 6 mice; PirB-/-: 4.262 ± 0.179; n = 18 cells / 7 mice; p = 0.0003, Mann-Whitney).

(K) mEPSC amplitudes were not significantly different between WT and PirB-/- mice (WT: 13.050 ± 0.671; n = 17 cells / 6 mice; PirB-/-: 12.737 ± 0.484; n = 18 cells / 7 mice; p = 0.5860, Mann-Whitney).

(L) The frequency of mIPSCs was significantly increased (decreased inter-event interval) in PirB-/- mice, compared to WT littermates (WT: 8.910 ± 0.431; n = 16 cells / 7 mice; PirB-/-: 10.611 ± 0.259; n = 18 cells / 7 mice; p = 0.0028, Mann-Whitney).

(M) mIPSC amplitudes were not significantly different between WT and PirB-/- mice (WT: 22.816 ± 0.748; n = 16 cells / 7 mice; PirB-/-: 24.228 ± 0.757; n = 18 cells / 7 mice; p = 0.2079, Mann-Whitney).

(N) Summary of WT and PirB-/- animal weights throughout the behavioral paradigm. Food restriction began at day -4 and the first training session began day 1. Both WT and PirB-/- mice rapidly dropped to 90% starting body weights, and there were no significant fluctuations in body weight throughout training (WT: n = 12; PirB-/-: n = 10; p = 0.907, 2-way repeated measures ANOVA).

(O) Baseline-normalized weights for tamoxifen-injected and control animals. There were no significant fluctuations in body weight throughout training (oil: n = 9; tamoxifen: n = 10; p = 0.700, 2-way repeated measures ANOVA).

(P) Experimental timeline for tamoxifen-injected animal training. CaMKII-CreER;PirB$^{fl/fl}$ mice received 5 consecutive days of tamoxifen (4 mg / day, or oil vehicle control) such that the last injection was ~1 week before food restriction and ~2 weeks before the first training day. Animals were retested 30 days following initial training in order to assess long-term memory of the newly acquired motor skill.
(B-D, N, O) Squares depict mean (± s.e.m.) within each genotype / condition.
(J-M) Circles represent individual cells. Box plots and mean ± s.e.m. are shown.
* $p < 0.05$, ** $p < 0.01$, *** $p < 0.001$; ns: non-significant.

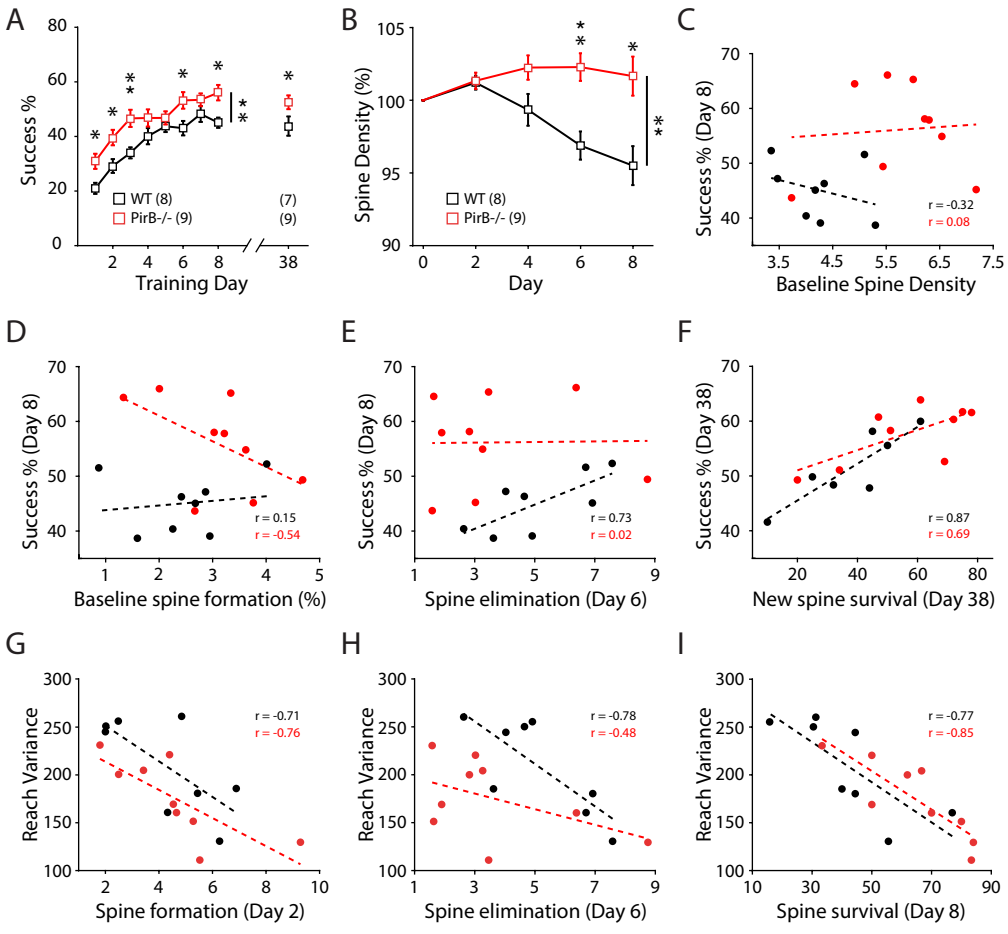

Albarran et al.,- Figure S2

Figure S2 (related to Figure 2). Relationship between spine dynamics and motor learning

(A) Mice were trained for 8 days followed by retesting at day 38. As before, PirB-/- mice performed the reaching task better compared to WT during 8 training days (WT: n = 8; PirB-/-: n = 9; p = 0.001, 2-way repeated measures ANOVA) and again when re-assessed 30 days after training (WT: X ± X%; n = 7; PirB-/-: X ± X%; n = 9; p = 0.031, Mann-Whitney).

(B) Spine density throughout training (normalized to the last baseline day) is significantly elevated in PirB-/- mice (WT: n = 8; PirB-/-: n = 9; p = 0.001, 2-way repeated measures ANOVA). Individual day statistics (day 2, WT: 101.21 ± 0.17%, PirB-/-: 101.34 ± 0.19%, p = 0.9996; day 4, WT: 99.34 ± 0.39%, PirB-/-: 102.25 ± 0.28%, p = 0.1983; day 6, WT: 96.88 ± 0.34%, PirB-/-: 102.28 ± 0.32%, p = 0.0049; day 8, WT: 95.59 ± 0.47%, PirB-/-: 101.66 ± 0.45%, p = 0.0216, Sidak posthoc multiple comparisons).

(C) Correlation between baseline spine density and last day performance on reaching task (WT: r = -0.3193; n = 8; p = 0.4407, Pearson correlation; PirB-/-: r = 0.0798; n = 9; p = 0.8382, Pearson correlation).

(D) Correlation between baseline spine formation and last day performance on reaching task (WT: r = 0.1490; n = 8; p = 0.7247, Pearson correlation; PirB-/-: r = -0.5435; n = 9; p = 0.1304, Pearson correlation).

(E) Correlation between day 6 spine elimination and last day performance on reaching task (WT: r = 0.7255; n = 8; p = 0.0416, Pearson correlation; PirB-/-: r = 0.0154; n = 9; p = 0.9687, Pearson correlation).

(F) Correlation between new spine survival on day 38 and day 38 performance on reaching task (WT: r = 0.8746; n = 7; p = 0.0100, Pearson correlation; PirB-/-: r = 0.6919; n = 9; p = 0.0389, Pearson correlation).

(G) Correlation between spine formation on day 2 and last day reach trajectory variance (WT: r = -0.7110; n = 8; p = 0.0480, Pearson correlation; PirB-/-: r = -0.7620; n = 9; p = 0.0169, Pearson correlation).

(H) Correlation between spine elimination on day 6 and last day reach trajectory variance (WT: r = -0.7778; n = 8; p = 0.0231, Pearson correlation; PirB-/-: r = -0.4760; n = 9; p = 0.1953, Pearson correlation).

(I) Correlation between new spine survival on day 8 and last day reach trajectory variance (WT: r = -0.7665; n = 8; p = 0.0265, Pearson correlation; PirB-/-: r = -0.8461; n = 9; p = 0.0040, Pearson correlation).

(A-C) Squares depict mean (± s.e.m.) within each genotype. * $p < 0.05$, ** $p < 0.01$.

(D-I) Circles depict individual animals, dotted lines depict linear fit of each correlation.

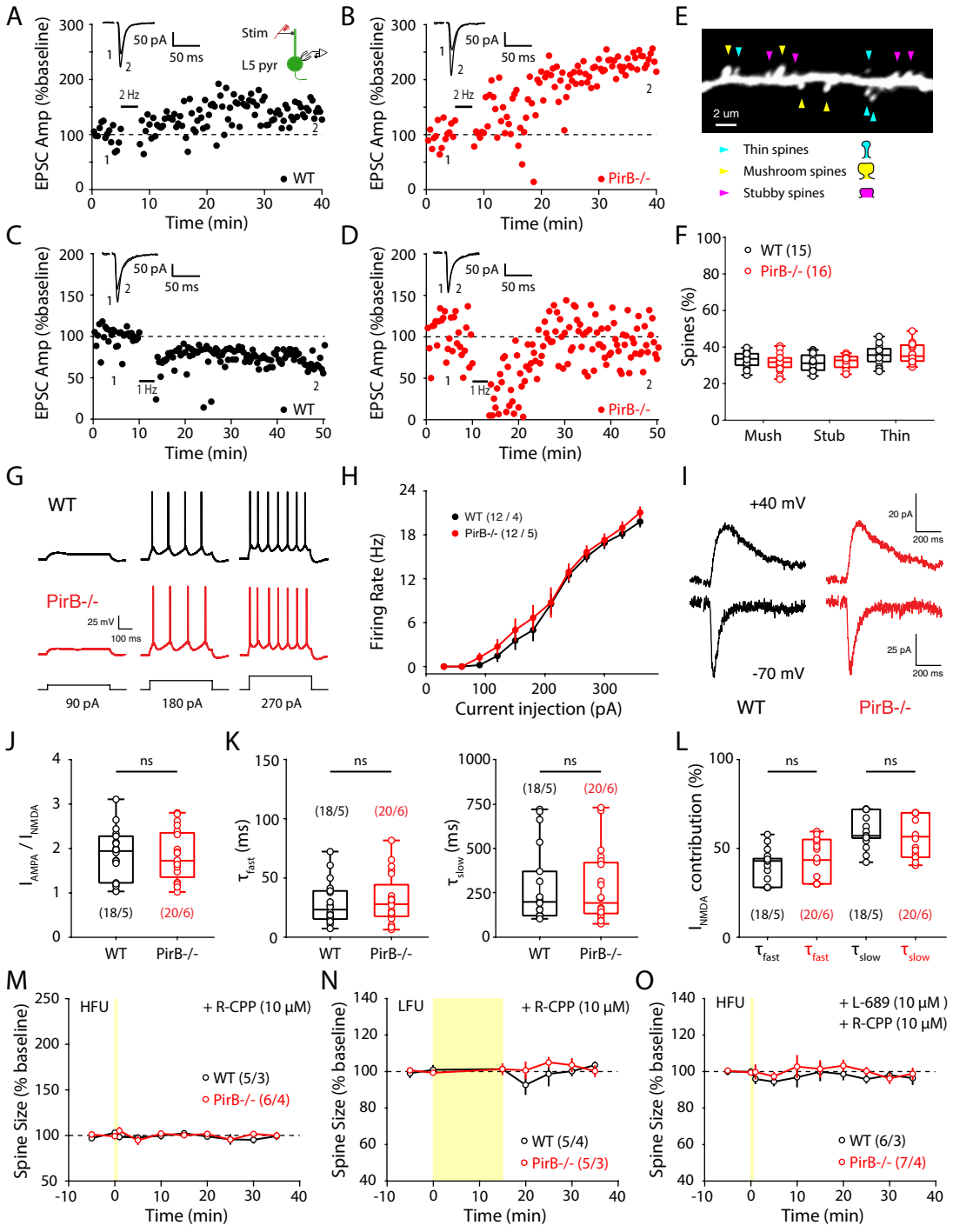

Albarran et al.,- Figure S3

Figure S3 (related to Figure 3). Long term synaptic plasticity, spine type, AMPA/NMDAR ratio, spine growth and shrinkage in WT and PirB-/- mice

(A, B) Representative whole-cell patch clamp recordings of layer 5 pyramidal neurons from acute coronal slices from WT (A) and PirB-/- (B) mice depicting evoked EPSC amplitudes before and after 2 Hz LTP induction.

(C, D) Representative recordings from WT (C) and PirB-/- (D) mice depicting evoked EPSC amplitudes before and after 1 Hz LTD induction.

(A-D) Average traces are shown for baseline (black) and end of recording (red), where each is the average of the last 5 minutes of their period (15 traces).

(E) Representative image of Thy1-YFP+ dendrite and dendritic spines. Arrowheads denote the spine type (yellow: mushroom; magenta: stubby; cyan: thin).

(F) Proportion of spine types present on dendrites do not differ between WT and PirB-/- mice (WT: 32.9 ± 1.2% mushroom, 31.38 ± 1.2% stubby, 35.74 ± 1.5% thin; n = 15 mice; PirB-/-: 31.74 ± 1.2% mushroom, 31.80 ± 1.0% stubby, 36.46 ± 1.4% thin; n = 16 mice; p = 0.986, p = 0.999, p = 0.998, 2-way ANOVA with multiple comparisons).

(G) Representative recordings of WT and PirB-/- layer 5 pyramidal neurons following current injections of 90, 180, and 270 pA in amplitude.

(H) No significant difference in firing rates between WT and PirB-/- cells across a range of current injections (WT: n = 12 cells / 4 mice; PirB-/-: n = 12 cells / 5 mice; p = 0.519, 2-way repeated measures ANOVA).

(I) Representative traces of evoked AMPAR (bottom) and NMDAR (top) currents isolated at -70 mV and +40 mV respectively.

(J) No difference in the ratio of I_{AMPA} to I_{NMDA} between WT and PirB-/- recorded cells (WT: 1.87 ± 0.14; n = 18 cells / 5 mice; PirB-/-: 1.84 ± 0.13; n = 20 cells / 6 mice; p = 0.804, Mann-Whitney).

(K) Left: fast decay time constants for I_{NMDA} responses are not different between WT and PirB-/- cells (WT: 28.88 ± 4.25 ms; PirB-/-: 31.66 ± 4.72 ms; p = 0.693, Mann-Whitney).

Right: slow decay time constants for I_{NMDA} responses are not different between WT and PirB-/- cells (WT: 287.16 ± 51.29 ms; PirB-/-: 276.88 ± 44.58 ms; p = 0.942, Mann-Whitney).

(L) No difference in the relative contributions of fast (WT: 39.89 ± 2.21%; PirB-/-: 42.86 ± 2.74%; p = 0.236, Mann-Whitney) or slow (WT: 60.11 ± 2.21%; PirB-/-: 57.14 ± 2.74%; p = 0.236, Mann-Whitney) decay time constants to I_{NMDA} responses of WT and PirB-/- cells.

(M) WT and PirB-/- spines targeted with HFU in the presence of R-CPP (10 μM) do not undergo significant spine growth (WT + R-CPP: n = 5 spines / 3 mice; baseline vs. 35 mins., p = 0.548, 2-way repeated measures ANOVA; PirB-/- + R-CPP: n = 6 spines / 4 mice; baseline vs. 35 mins., p = 0.937, 2-way repeated measures ANOVA).

(N) WT and PirB-/- spines targeted with LFU in the presence of R-CPP (10 μM) do not undergo significant spine shrinkage (WT + R-CPP: n = 5 spines / 4 mice; baseline vs. 35 mins., p = 0.691, 2-way repeated measures ANOVA; PirB-/- + R-CPP: n = 5 spines / 3 mice; baseline vs. 35 mins., p = 0.841, 2-way repeated measures ANOVA).

(O) WT and PirB-/- spines targeted with HFU in the presence of L-689 (10 μM) and R-CPP (10 μM) do not undergo significant spine shrinkage (WT + L-689 + R-CPP: n = 6 spines / 3 mice; baseline vs. 35 mins., p = 0.589, 2-way repeated measures ANOVA; PirB-/- + L-689 + R-CPP: n = 7 spines / 4 mice; baseline vs. 35 mins., p = 1.000, 2-way repeated measures ANOVA).

(A-D) Circles represent individual EPSC amplitudes (normalized to baseline).

(F) Circles represent individual mice. Box plots and mean ± s.e.m. are shown.

(H) Circles represent mean firing rates ± s.e.m. across all recorded cells.

(J-L) Circles represent individual recorded cells. Box plots and mean ± s.e.m. are shown.

(M-O) Circles represent mean spine volumes ± s.e.m.

ns: non-significant.

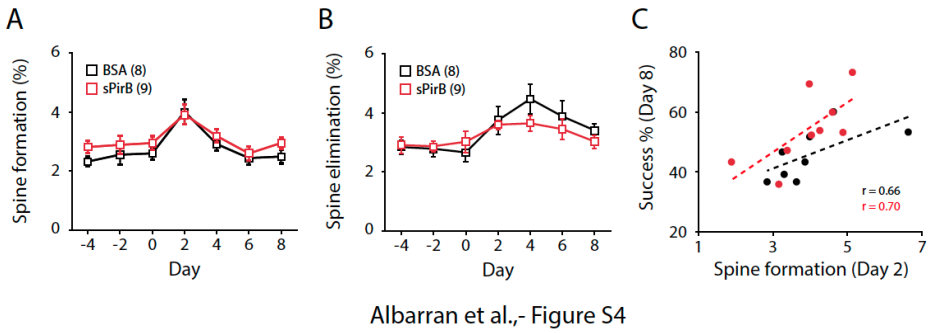

Figure S4 (related to Figure 4). Spine dynamics in WT mice infused with sPirB

(A) Spine formation rates throughout training in BSA or sPirB infused mice were not significantly different ($p = 0.1166$, 2-way repeated measures ANOVA).

(B) Spine elimination rates throughout training in BSA or sPirB infused mice were not significantly different ($p = 0.3813$, 2-way repeated measures ANOVA).

(C) Correlation between new spine formation on day 2 and last day performance on reaching task (WT: $r = 0.6583$; $n = 8$; $p = 0.0759$, Pearson correlation; PirB-/-: $r = 0.6978$; $n = 9$; $p = 0.0366$, Pearson correlation).

(A, B) Squares depict mean (± s.e.m.) within each genotype.

(C) Circles depict individual animals, dotted lines depict linear fit of each correlation.